NON-SMOOTH SPATIO-TEMPORAL COORDINATES IN NONLINEAR DYNAMICS

V.N. Pilipchuk
Wayne State University
Detroit, MI 48202

January 25, 2011

Abstract

This paper presents an overview of physical ideas and mathematical methods for implementing non-smooth and discontinuous substitutions in dynamical systems. General purpose of such substitutions is to bring the differential equations of motion to the form, which is convenient for further use of analytical and numerical methods of analyses. Three different types of nonsmooth transformations are discussed as follows: positional coordinate transformation, state variables transformation, and temporal transformations. Illustrating examples are provided.

1 Introduction

Discontinuities of states in physical models often represent the result of intentional idealization of abrupt but still smooth changes in dynamical characteristics. Such idealizations help to skip complicated details of modeling on relatively small intervals of the dynamics. From the mathematical standpoint however, every discontinuity of states breaks the system and thus increases the system dimension as many as twice even though the equations may remain the same before and after the discontinuity. This work will outline and illustrate different ideas of preventing the dimension increase while dealing with discontinuities of system states. Regardless physical principals and mathematical specifics, preliminary modification of descriptive functions represents a common feature of such approaches. Note that many analytical methods dealing with dynamical systems preliminarily adapt the equations of motions through different substitutions and transformations in order to ease further steps of analyses. Although a universal recipe for such substitutions is rather difficult to suggest, there are some general principles to follow. For instance, classes of transformations should comply with classes of systems considered. The term *classes* remains intentionally unspecified here since it may indicate any generic feature of the model, such as linearity or nonlinearity, a class of smoothness, or other mathematical prop-

erties. In particular, this work focuses on substitutions including nonsmooth or discontinuous functions.

Generally speaking, differential operations with nonsmooth functions require generalized interpretations of equalities as integral identities, in other words, in terms of distributions [50]. In linear cases, such interpretations are usually quite straightforward since distributions represent linear functionals [67]. Nonlinear models however impose certain structural constraints on the presence of nonsmooth or discontinuous functions in differential equations [14], [15]. Moreover, whether or not some combinations of discontinuous functions are meaningful may depend upon physical contents of variables participating in such combinations [35]. From the mathematical standpoint, physical interpretations allow for narrowing families of smooth functions that have discontinuities in their asymptotic limits. As a result, some combinations of discontinuous functions may acquire certain meanings of distributions. To this end, some introductory remarks on transitions to nonsmooth or discontinuous limits in nonlinear cases will be introduced. For that reason, consider, for instance, the following product of the Heaviside' unit-step function and the Dirac' delta-function, $\theta(t-1)\delta(t-1)$. Generally speaking, such a 'product' is undefined due to the discontinuity of $\theta(t-1)$. In other words, no certain number can be prescribed to the integral $\int_{-\infty}^{\infty}\theta(t-1)\delta(t-1)dt$, unless it is known what kind of processes both functions actually represented before their transition to discontinuous limits. For illustrating purposes, let $\delta_\varepsilon(t-1) = \varepsilon^{-2}\cosh^{-2}[(t-1)/\varepsilon^2]/2$ be the force applied to a unit mass whose velocity is zero at $t=-\infty$. Then the velocity is described by $v(t) = \theta_\varepsilon(t-1) \equiv (1+\tanh[(t-1)/\varepsilon^2])/2$ due to the relationship $\dot{\theta}_\varepsilon(t-1) = \delta_\varepsilon(t-1)$; see Fig. 1 for illustration.

Based on standard definitions, it can be shown that, in terms of weak limits, $\delta_\varepsilon(t-1)$ gives $\delta(t-1)$ whereas $\theta_\varepsilon(t-1)$ gives $\theta(t-1)$ as $\varepsilon \to 0$. Note that the above choice for $\delta_\varepsilon(t-1)$ is not unique - there are many other cases leading to the same result. Regardless magnitude of ε, however, the work done by this force is calculated as follows

$$\begin{aligned}
\int_{-\infty}^{\infty}\theta_\varepsilon(t-1)\delta_\varepsilon(t-1)dt &= \\
\int_{-\infty}^{\infty}\theta_\varepsilon(t-1)\dot{\theta}_\varepsilon(t-1)dt &= \frac{1}{2}[\theta_\varepsilon(t-1)]^2|_{-\infty}^{\infty} = \frac{1}{2}
\end{aligned}$$

Therefore, transition to the limit $\varepsilon \to 0$ gives

$$\int_{-\infty}^{\infty}\theta(t-1)\delta(t-1)dt = \frac{1}{2} = \frac{1}{2}\int_{-\infty}^{\infty}\delta(t-1)dt$$

In terms of distributions, the above expression means[1]

$$\theta(t-1)\delta(t-1) = \frac{1}{2}\delta(t-1) \tag{1}$$

[1]Strictly speaking, a so-called testing function must be added to the integrands as a factor in order to completely prove this statement.

The left-hand side in (1) can be interpreted as a mechanical power generated by the impact force $\delta(t-1)$. To some extent, the result (1) is based on the common sense that such a power must exist regardless mathematical ambiguity of the left-hand side of identity (1). Note that interpretation (1) becomes possible due to the 'constraint' coupling the two functions, $\dot{\theta}_{\varepsilon}(t-1) = \delta_{\varepsilon}(t-1)$, which is supposed to hold in the limit case $\varepsilon \to 0$,

$$\dot{\theta}(t-1) = \delta(t-1) \tag{2}$$

were the over dot means Schwartz derivative.

This standard relationship of the theory of distributions as well as its different variations will be used below. Relationship (1) may also serve as a basis for other definitions, for instance,

$$\mathtt{sgn}(t-1)\delta(t-1) = 0 \tag{3}$$

where $\mathtt{sgn}(t-1) = 2\theta(t-1) - 1$.

While using (1) or (3), both functions $\theta(t-1)$ and $\delta(t-1)$ must be considered together with their 'smooth prehistories' generated by the same family of smooth functions $\delta_{\varepsilon}(t-1)$. If the limit functions $\theta(t-1)$ and $\delta(t-1)$ are based on different families of smooth functions then relationships (1) or (3) may not hold; see the next section for more details.

To conclude this, as follows from the above remarks, despite of the universal notations, discontinuous functions may still inherit some features of the generating families of smooth functions. Therefore, analytical manipulations with discontinuous and delta-functions must account for both physical content of the problem and mathematical structure of equations. In the most direct way, such complications can be avoided by considering models on different time intervals and introducing appropriate matching conditions for the corresponding pieces of solutions. In many cases, however, the matching times are a priori unknown and must also be determined from the same matching conditions. As mentioned at the beginning, this work gives an overview of another approaches satisfying the matching conditions automatically through specific non-smooth transformations of variables. Briefly, the paper is organized as follows: 1) Caratheodori equations and discontinuous substitutions [14] for systems under external pulses and wave propagation problems, 2) non-smooth coordinate space transformations for impact systems with elastic perfectly stiff constraints and possible extensions on non-elastic constraints [69], [70], [71], 3) non-smooth state (phase) space transformation [21], [24], [23] and applications to modeling the impact dynamics with an arbitrary coefficient of restitution, 4) non-smooth temporal transformations [40], [41] for periodic and non-periodic motions, analytical and semi-analytical tools, unstable periodic and chaotic motions, 5) different combined approaches [60], [13], [43].

2 Nonsmooth coordinate transformations

2.1 Dynamical systems with distributions included as summands: linear discontinuous transformations

Different classes of differential equations, linear and nonlinear, with additively involved distributions were considered Filippov [14]. In particular, the methods of reducing such equations to Caratheodori equations were described. Briefly, such methods eliminate distributions from the differential equations based on predictions for local dynamical effects of the distributions. Such effects are simply included into the corresponding substitutions so that new equations are free of singular terms and thus satisfy the so-called Caratheodory conditions. As a result, it is possible to prove existence and investigate different properties of solutions. Such a generalization is based on the integral form of the differential equation $\dot{x} = f(t, x)$ with a continuous right-hand side

$$x(t) = x(t_0) + \int_0^t f(s, x(s))ds \tag{4}$$

If the function $f(t, x)$ is discontinuous in t, but still continuous in x, then the functions satisfying (4) can be considered as solutions of the equation $\dot{x} = f(t, x)$. Generally, integration in (4) should comply with the concept of Lebesgue integral. In this case, the function $f(t, x)$ does not have to be pointwise defined[2]. However, the following Caratheodory conditions must be satisfied: In the domain D of the (t, x)-space, the function $f(t, x)$ is 1) defined and continuous in x for almost all t, 2) measurable in t for each x, and 3) the estimate $|f(t, x)| \leq m(t)$ holds, where $m(t)$ is a summable function on each finite interval, if t is not bounded in D.

As a simplified illustration, let us consider a single degree-of-freedom system whose velocity, $v = v(t)$, is described by the differential equation

$$\dot{v} + kv^3 = q\delta\,(t - t_1) \tag{5}$$

where k, q and t_1 are constant parameters, and δ is the Dirac'delta function.

Equation (5) describes a unit-mass particle in a nonlinearly viscous media with the cubic dissipation law. In this case, the δ-input generates a step-wise discontinuity of the response $v(t)$ at $t = t_1$, nevertheless the nonlinear operation in (5) remains meaningful. Moreover, the δ-pulse can be eliminated from equation (5) as follows. Since the velocity must be bounded, then only the inertia term can compensate the impact force on the right-hand side of equation (5). In other words, near the impact time $t = t_1$, equation (5) is linearized as $\dot{v} = q\delta\,(t - t_1)$. Comparing this with equation (2), gives solution

$$v = u + q\theta\,(t - t_1) \tag{6}$$

[2]Practically, such an extension almost never contradicts to the physical contents of modeling; recall that the differential equations of motion are derived from variational principles formulated in the integral form.

where u is an arbitrary constant.

Let us assume now that u is a function of time $u = u(t)$ such that solution (6) becomes valid for the original equation (5) on the entire time interval, $-\infty < t < \infty$. Then, substituting (6) in (5), and taking into account that $\dot{\theta}(t - t_1) = \delta(t - t_1)$ and $\theta^2(t - t_1) = \theta(t - t_1)$, gives

$$\dot{u} + k[u^3 + (q^3 + 3uq^2 + 3u^2 q)\theta(t - t_1)] = 0 \tag{7}$$

In contrast to (5), equation (6) includes no δ-function and thus admits visualization of its phase flow on the (t, v)-plane with the related qualitative study.

Note that substitution (6) generalizes on equation

$$\dot{v} = f(v, t) + \sum_{i=1}^{\infty} q_i \delta(t - t_i) \tag{8}$$

where $f(v, t)$ is assumed to have no singularities within some domain of the (v, t)-plane, and $\{q_i\}$ and $\{t_i\}$ are constants.

In this case, the following substitution eliminates all the δ-functions from equation (8)

$$v(t) = u(t) + \sum_{i=1}^{\infty} q_i \theta(t - t_i) \tag{9}$$

Further generalization on the vector-form equations is quite obvious. Complications may occur however when the structure of original equations is changed as described in the next section.

2.2 Distributions as parametric inputs in dynamical systems

This specific case illustrates the major issue of using distributions for modeling dynamical systems. Following reference [14], consider the linear initial value problem

$$\begin{aligned} \dot{v} + k\delta(t - t_1)v &= 0 \\ v(0) &= v_0 \end{aligned} \tag{10}$$

where k and $t_1 > 0$ are constant.

Since $\dot{v} = 0$ for $t < t_1$ and $t > t_1$, then

$$v = v_0[1 - \lambda\theta(t - t_1)] \tag{11}$$

where λ is yet unknown constant parameter of discontinuity such that $v = v_0$ for $t < t_1$ and $v = -\lambda v_0$ for $t > t_1$.

Equation (10) shows that the jump of the solution depends on the behavior of solution itself near the point $t = t_1$. In this case, there is no certain choice for λ since its magnitude depends upon additional assumptions regarding the

model [14]. To clarify the details, let us substitute (11) in (10) with the intent to find λ. This gives

$$(k-\lambda)\delta(t-t_1) - k\lambda\theta(t-t_1)\delta(t-t_1) = 0 \tag{12}$$

It was mentioned in Introduction that the combination $\theta(t-t_1)\delta(t-t_1)$ has no certain meaning in the distribution theory. However, the form of (11) together with equation (10) dictate

$$\theta(t-t_1)\delta(t-t_1) = \alpha\delta(t-t_1) \tag{13}$$

and therefore,

$$\lambda = \frac{k}{1+\alpha k} \tag{14}$$

where the magnitude of parameter α depends on the model' assumptions.

For instance, the number $\alpha = 1/2$ was obtained in introductory example (1). In the present case, it is unknown whether the functions $\theta(t-t_1)$ and $\delta(t-t_1)$ are generated by the same family of smooth functions. Nevertheless, physical approaches to determining α may be similar to that described in Introduction. Namely, let us replace the Dirac function $\delta(t-t_1)$ in equation (10) by its smooth preimage $\delta_\varepsilon(t-t_1)$ defined in Introduction. As a result, equation (10) takes the form of a regular separable equation whose solution is

$$v = v_0 \exp\left[-\frac{1}{2}k\left(\tanh\frac{1}{\varepsilon^2} + \tanh\frac{t-t_1}{\varepsilon^2}\right)\right] \tag{15}$$

This gives

$$v = v_0\left\{1 - [1-\exp(-k)]\theta(t-t_1)\right\} \quad \text{as} \quad \varepsilon \to 0 \tag{16}$$

Comparing (16) to (11) and taking into account (14), gives $\lambda = 1-\exp(-k)$ and therefore

$$\alpha = \frac{1}{1-\exp(-k)} - \frac{1}{k} \tag{17}$$

Expression (17) shows that definition (13) depends upon the model parameter k; see Fig. 2 for illustration. In particular, $\alpha \to 1/2$ as $k \to 0$, and this brings us back to the case considered in Introduction.

Finally, note that substitutions of type (6) and (9) as well as its different variations are widely used in the literature to describe moving discontinuity waves [68], [35], [17]. In most such cases though there is no explicit source of discontinuities that naturally occur as a result of wave shape evolutions predetermined by initial perturbations and inner properties of wave model.

2.3 Nonsmooth positional coordinates

The idea of nonsmooth coordinates associates with elastic but perfectly stiff barriers reflecting moving particles in a mirror-wise manner. Since outcome of

such reflections is predictable then it can be built into the mechanical model in advance through the corresponding nonsmooth coordinate transformations. It was shown in references [69], [70], and [71] that introducing nonsmooth coordinates simply eliminates barriers by unfolding the configuration space to include the area behind the barrier. As a result, the differential equations of motion are derived on the entire time interval with no need in formulation of impact conditions. For illustrating purposes, consider the following N-degree-of-freedom Lagrangian system

$$
\begin{aligned}
L &= \frac{1}{2}\sum_{i=1}^{N}\dot{q}_i^2 - \sum_{i=0}^{N}k_i(q_{i+1}-q_i)^2 && (18)\\
|q_i(t)| &\leq 1 && (19)\\
q_0(t) &\equiv q_{N+1}(t) \equiv 0 && (20)
\end{aligned}
$$

This is a chain of unit-mass particles connected by linearly elastic springs of stiffness k_i. Perfectly stiff elastic constraints are imposed on each of the coordinates according to (19). Although Lagrangian (18) generates linear differential equations, these equations alone do not describe the entire system. Due to the presence of constraints (19), the system is actually strongly nonlinear that becomes obvious in adequately chosen coordinates. Transition to such coordinates is described by

$$q_i = \tau(x_i) \tag{21}$$

where τ is the triangular sine-wave

$$
\begin{aligned}
\tau(x) &= \frac{2}{\pi}\arcsin\sin\frac{\pi x}{2} = \begin{cases} x & \text{for } -1 \leq x \leq 1 \\ -x+2 & \text{for } 1 \leq x \leq 3 \end{cases} && (22)\\
&\tau(x) \overset{\forall x}{=} \tau(4+x)
\end{aligned}
$$

Note that notation (22) and normalization of the period differ from those introduced in original works [69], [70], [71]. The only reason for such modification is to deal with the triangular wave of unit slope[3]

$$[\tau'(x)]^2 = 1 \tag{23}$$

for at least almost all x.

The coordinate transformation (21) brings system (18) through (20) to the form

$$
\begin{aligned}
L &= \frac{1}{2}\sum_{i=1}^{N}\dot{x}_i^2 - \sum_{i=0}^{N}k_i[\tau(x_{i+1})-\tau(x_i)]^2 && (24)\\
x_0(t) &\equiv x_{N+1}(t) \equiv 0 && (25)
\end{aligned}
$$

[3] Although this condition does no matter for the method introduced in references [69], [70], [71], Section 3 of the present paper describes another method for which normalization (23) is essential.

It is seen from (24) that transformation (22) preserves the quadratic form of kinetic energy while the constraint conditions (19) are satisfied automatically due to the property $|\tau(x)| \leq 1$. In contrast to (18), Lagrangian (24) completely describes the model on the entire time interval $0 \leq t < \infty$. However, in terms of the new coordinates x_i, the potential energy acquired a non-local cell-wise structure so that the corresponding differential equations of motion are essentially nonlinear; for example, see (26) below. Now every impact interaction with constraints is interpreted as a transition from one cell to another as illustrated below on the two degrees-of-freedom model, $N = 2$. In this case, Lagrangian (24) gives the differential equations of motion on the infinite plane $-\infty < x_i < \infty$ $(i = 1, 2)$ with no constraints

$$\begin{aligned} \ddot{x}_1 + [(k_0 + k_1)\tau(x_1) - k_1\tau(x_2)]\tau'(x_1) &= 0 \\ \ddot{x}_2 + [(k_1 + k_2)\tau(x_2) - k_1\tau(x_1)]\tau'(x_2) &= 0 \end{aligned} \tag{26}$$

Fig. 3 shows the corresponding equipotential energy levels and a sample trajectory of beat-wise dynamics represented by Figs.4 and 5 in the original coordinates. Fig. 3 shows, for instance, that the system is trapped in some cells for the energy exchange process. After one of the two masses accumulated the energy, which is sufficient to reach the barrier, the impact event happens accompanied transition to another cell. The fact of energy exchange inside a trapping cell is confirmed by the transversality of incoming and outcoming pieces of the trajectory. As long as the mass remains in impact regime, its trajectory is passing through one cell to another until the system is trapped again in rather another cell for a new energy exchange process. A similar geometrical interpretation but for impact mode dynamics was introduced earlier in [65], where the impact modes were associated with 'hidden geometrical symmetries' revealed by periodic patterns of equipotential lines as shown in Fig. 6.

In particular, closed form analytical solutions for different impact modes were obtained by means of the averaging procedure. Note that, according to the original works [69], [70], [71], applicability of the averaging procedure constitutes the major advantage given by transformation (21) since infinite impact forces are effectively eliminated from the system.

Similar kind of visualization for a two-degree-of-freedom vibrating system with only one mass under two-sided constraint condition was used in [46].

Let us consider a one-degree-of-freedom unit mass oscillator with the potential energy of restoring force $P(q)$,

$$L = \frac{1}{2}\dot{q}^2 - P(q) \tag{27}$$

whose motion is limited by the interval

$$-1 \leq q \tag{28}$$

It is assumed that the oscillator collides with a one-sided perfectly stiff barrier at $q = -1$ with no energy loss. In this case, the constraint (28) is eliminated

by the space unfolding coordinate transformation $q \to x$:

$$q = -1 + |x + 1| \tag{29}$$

where the constant shifts in (29) are chosen to preserve the origin and barrier positions.

Substituting (29) in (27), gives

$$L = \frac{1}{2}\dot{x}^2 - P(|x + 1| - 1) \tag{30}$$

The system' phase trajectories are described by the energy integral $\dot{x}^2/2 + P(|x+1|-1) = Const$. This family of curves is illustrated by Fig. 7 on the phase plane $x\dot{x}$ at different energy levels in the case $P(q) = q^2/2$. In particular, it is seen that high-energy trajectories are non-smooth due to mirror-wise reflections against the barrier at $x = -1$ ($q = -1$). As a result, the phase portrait of the oscillator has effectively non-local structure, where any transition from one side of the plane to another is the result of impact interaction with the barrier.

Although original works [69], [70], [71], deal with illustrating models of deterministic dynamics, further applications were shifted mostly into the area of random vibrations may be due to earlier works [9] and [12]. Different analytical and numerical tools in this area were developed during recent few years; see references [38], [10], [11], [51]. From the standpoint of practical applications, inelastic effects of interactions with stiff constraints become essential. Generally, impact dissipation effects can be modeled by the dissipative term [71], [4], [11] $(1-\kappa)\dot{x}|\dot{x}|\delta_{-}(x)$, where $\delta_{-}(x)$ is a specific rule rather than conventional Dirac function. According to this rule, the impulsive damping acts right before the result of such damping namely velocity jump occurs. Such damping model is justified if the restitution coefficient κ is close to unity so that the factor $1-\kappa$ is small. In this case, the integral effect of the impulsive damping can play the role perturbation within asymptotic procedures, in which the velocity $\dot{x}$ is given by an unperturbed system and therefore remains continuous. Distributed viscous damping effects still can be described in a regular way by continuos terms as it was done, for instance, in [3]. Non-elastic impact interactions with constraints can be modeled also in a purely geometrical way under some conditions on the class of motions though [71].

Another approach that deals with the class of nonsmooth 'non-conservative' transformations is described in the next subsection.

2.4 Nonsmooth transformation of state variables

Generalized approaches to eliminating non-elastic constraints should obviously involve both types of the state variables - coordinates and velocities. For illustrating purposes, let us consider the case of harmonic oscillator under the constraint condition

$$\dot{\mathbf{x}} = \mathbf{A}\mathbf{x} \tag{31}$$

$$x_1 > 0 \tag{32}$$

where $\mathbf{x} = [x_1(t), x_2(t)]^T$ is the system' state vector such that $x_2 = \dot{x}_1$, and

$$\mathbf{A} = \left[\begin{array}{cc} 0 & 1 \\ -\omega^2 & 0 \end{array} \right] \tag{33}$$

It is also assumed that every collision with the constraint at $x_1 = 0$ is accompanied by a momentary energy loss characterized by the coefficient of restitution κ, in other words

$$x_2(t^* + 0) = -\kappa x_2(t^* - 0) \tag{34}$$

where t^* is the collision time, at which $x_1(\ t^*) = 0$.

The idea is to unfold the phase space in such way that the energy loss occurs automatically whenever the system crosses preimage of the line $x_1 = 0$. The corresponding non-conservative transformation was introduced in [21], [24], [23] as a transformation of state vector, $\mathbf{x} \longrightarrow \mathbf{y}$, of the form

$$\mathbf{x} = \mathbf{S}\mathbf{y} \tag{35}$$

where $\mathbf{y} = [s(t), v(t)]^T$ is a new state vector, and the transition matrix is given by

$$\mathbf{S} = \left[\begin{array}{cc} 1 & 0 \\ 0 & 1 - k\mathrm{sgn}(sv) \end{array} \right] \mathrm{sgn}(s) \tag{36}$$

where $k = (1 - \kappa)/(1 + \kappa)$.

Note that transformation (35) is strongly nonlinear due to the nonsmooth dependence $\mathbf{S} = \mathbf{S}(\mathbf{y}, k)$. Nevertheless, substitution (35), gives equation

$$\dot{\mathbf{y}} = (\mathbf{S}^{-1}\mathbf{A}\mathbf{S})\mathbf{y} \tag{37}$$

There is some 'hidden issue' with substitution (35) since the result (37) has the same form as it would have in the case of constant matrix $\mathbf{S}$. In fact, the matrix $\mathbf{S}$ is constant just almost everywhere. A formal substitution of (35) in (31) would eventually impose specific conditions on distributions similar to (3).

In the component-wise form, expressions (35) and (37) are written as, respectively,

$$\begin{aligned} x_1 &= x_1(s, v) \equiv s\mathrm{sgn}(s) \\ x_2 &= x_2(s, v) \equiv \mathrm{sgn}(s)[1 - k\mathrm{sgn}(sv)]v \end{aligned} \tag{38}$$

and

$$\begin{aligned} \dot{s} &= [1 - k\mathrm{sgn}(sv)]v \\ \dot{v} &= -\omega^2 s[1 + k\mathrm{sgn}(sv)]/(1 - k^2) \end{aligned} \tag{39}$$

Now both unknown components of the state vector are continuous, whereas effects of non-elastic collisions (34) are captured by transformation (38).

Finally, consider the general case of one-degree-of-freedom nonlinear oscillator

$$\begin{aligned} \dot{x}_1 &= x_2 \\ \dot{x}_2 &= -f(x_1, x_2, t) \end{aligned} \tag{40}$$

whose motion is restricted to the positive half plane $x_1 > 0$ by a non-elastic barrier at $x_1 = 0$ of the restitution coefficient κ.

Applying transformation (38) to system (40), gives

$$\begin{aligned} \dot{s} &= [1 - k\mathrm{sgn}(sv)]v \\ \dot{v} &= -f(x_1(s,v), x_2(s,v), t)\mathrm{sgn}(s)[1 + k\mathrm{sgn}(sv)]/(1-k^2) \end{aligned} \tag{41}$$

Although the technique is illustrated on a one-degree-of-freedom model, similar coordinate transformations apply to multiple degree-of-freedom systems by choosing one of the coordinates perpendicular to the constraint. For that reason, it is convenient to use the Routh descriptive function whose normal to the constraint coordinate is Lagrangian whereas other coordinates and associated momenta are Hamiltonian [24].

Finally, note that adjustments of classes of smoothness of dynamical systems by eliminating infinite discontinuities extend the set of applicable analytical tools. For instance, problems of stability and bifurcation analyses of impact motions were considered in [24] by means of the linearization technique developed for dynamical systems with nonsmooth right-hand sides [2]. In particular, the fundamental matrix of explicit form and the corresponding characteristic equations were obtained. As a result, investigation of stability and bifurcations became possible by using conventional methods. In fact, before the transformation, discontinuities of phase trajectories as those shown in Fig. 9 would complicate any local analyses. However, the transformation improves the class of smoothness to the extent which is needed to build major objects of local analyses and averaging tools. A regular approach to stability and bifurcation analysis in impact systems was proposed in [22]. In particular, it was shown that the discontinuous bifurcation of grazing impact can be regularized. This may lead to a new interpretation of grazing bifurcations. Namely, after such bifurcation, some periodic motion might survive and even preserve stability.

3 Nonsmooth temporal arguments

In this section, we describe nonsmooth substitutions of the independent variable, which is temporal argument in the present text. It will be shown below that such nonsmooth substitutions associate with some common temporal symmetries of motions regardless of types of systems. This approach was originally developed for the class of strongly non-linear but smooth oscillators [40], [41]. However, its main specifics are clearly seen even in the case of non-oscillatory motion of a classic unit-mass particle under returning potential force as shown in Figs. 10 and 11. *The idea is to employ most elementary macrodynamical processes*

whose specifics nevertheless provide sufficient conditions for observing strong nonlinearities [48]. Examples of such 'elementary strongly nonlinear processes' are found among the rigid-body motions as those shown in Fig. 12. However, the key question is how to bridge the gap between the classes of smooth and nonsmooth motions within the same mathematical formalism. It will be shown below on simple examples that nonsmooth substitutions of temporal argument may play the role of such a bridge.

3.1 Positive time

Let the potential energy $P(x)$ be a smooth function of the time dependent coordinate x as qualitatively shown in Fig. 10. Then the differential equation of motion of a unit-mass particle under the force $f(x) = P'(x)$ is given by

$$\ddot{x} + f(x) = 0 \tag{42}$$

The initial conditions are $x = x_0 > 0$ and $\dot{x} = v_0 < 0$ at $t = t_0 < 0$ as shown in Figs. 10 and 11.

As the particle reaches a turning point at some time $t = a$ it makes a U-turn. Since equation (42) admits the group $t \longrightarrow -t$, the reverse motion will be symmetric with respect to the U-turn point $t = a$. Such a 'prediction' builds into the differential equation of motion (42) through the new temporal argument $t \longrightarrow s$:

$$s = |t - a|, \quad x = x(s) \tag{43}$$

The mechanical model generating such time argument by its natural motion is shown in Fig. 12 (a). Since at almost all t,

$$\dot{s}^2 = 1 \tag{44}$$

then, substituting (43) in (42), gives

$$\frac{d^2x}{ds^2} + f(x) = 0, \quad s > 0 \tag{45}$$

under condition

$$\frac{dx}{ds} = 0 \quad \text{if} \quad s = 0 \tag{46}$$

It is easy to see that the boundary condition (46) eliminates singularity of second time derivative that formally occurs due to the non-smoothness of substitution (43).

As follows from Fig. 11, substitution (43) reverses the time direction exactly when the particle makes a U-turn. Although the form of the equation remains the same, substitution (43) gives certain advantages from both physical and mathematical standpoints. First, equation 45, even after being drastically simplified as $d^2x/ds^2 = 0$, still preserves the major dynamical event, which is the U-turn of the particle. In this degenerated case, the smooth potential barrier is effectively replaced by a perfectly stiff one as follows from the general solution,

$x = As(t) + B$, where A and B are arbitrary constants of integration. Now, if some perturbation series converges for $s \geq 0$, then it is automatically converges for the entire interval of the original time, $-\infty < t < \infty$.

As another example, let us consider the case of impulsively loaded single degree-of-freedom system,

$$\ddot{x} + f(x) = p\ddot{s} \tag{47}$$

where $\ddot{s} = 2\delta(t-a)$ and $p = const$.

Substituting (43) in (47) and taking into account (44), gives

$$\frac{d^2x}{ds^2} + f(x) = \left(p - \frac{dx}{ds}\right)\ddot{s} \tag{48}$$

Eliminating the singularity $p\ddot{s}$ in (48), gives the same equation (45) however under non-homogeneous boundary condition

$$\frac{dx}{ds} = p \quad \text{if} \quad s = 0 \tag{49}$$

Since substitution (43) is non-invertible in the form $t = t(s)$ on the entire time interval, then using the argument s in general case of dynamical system appears to be less straightforward but nevertheless possible based on the following identity

$$t = a + s\dot{s} \tag{50}$$

Due to relationship (44), the combination (50) represents a specific complex number with the basis $\{1, \dot{s}\}$ [45]. In contrast to the conventional elliptic complex algebra, the operation $1/t$ with (50) may not hold. Interestingly enough, such algebraic structures has been known for quite a long time [8], [61] mostly as abstract mathematical objects with no relation to nonsmooth functions or impact systems. In the modern mathematical literature, these numbers are often referred to as a simple example of Clifford algebras under the name 'hyperbolic algebra' [56] with very many synonyms though [1]. Some areas of physics are linked to this algebra quite closely [19], but constructive applications are rather limited.

Let us formulate useful algebraic properties of hyperbolic numbers adapted to the form (50). For instance, the hyperbolic conjugate to (50) is introduced as $t^- = a - s\dot{s}$, and the hyperbolic modulus is calculated as $|t|_h = \sqrt{|tt^-|} = \sqrt{|a^2 - s^2|}$. The term *hyperbolic* associates with the fact that the relationship $|t|_h = \rho$ with some fixed ρ describes a four branched hyperbola on the hyperbolic plane with the basis $\{1, \dot{s}\}$:

$$\begin{aligned} t &= \pm\rho(\cosh\phi + \dot{s}\sinh\phi) \equiv \pm\rho\exp(\dot{s}\phi), \quad \phi = \operatorname{arctanh}(s/a) \\ t &= \pm\rho(\sinh\phi + \dot{s}\cosh\phi) \equiv \pm\rho\exp(\dot{s}\phi), \quad \phi = \operatorname{arctanh}(a/s) \end{aligned}$$

The hyperbolic numbers create isomorphism with symmetric 2×2-matrixes, so that, for instance

$$(a + s\dot{s})^2 \longleftrightarrow \begin{pmatrix} a & s \\ s & a \end{pmatrix}^2 \tag{51}$$

Note that, in our case, the hyperbolic structure is generated by time dependent transformations rather than imposed on abstract elements by mathematical definitions. As a result, differential and integral properties of hyperbolic numbers can be introduced [45]. So, for practically any function $x\,(t)$, it can be shown that

$$x\,(t) = x\,(a + s\dot{s}) = X\,(s) + Y\,(s)\,\dot{s} \tag{52}$$

where

$$\begin{aligned} X\,(s) &= \frac{1}{2}\left[x\,(a+s) + x\,(a-s)\right] \\ Y\,(s) &= \frac{1}{2}\left[x\,(a+s) - x\,(a-s)\right] \end{aligned} \tag{53}$$

Then, taking into account (44), gives

$$\dot{x}\,(t) = Y'\,(s) + X'\,(s)\,\dot{s} + p\ddot{s} \tag{54}$$

where

$$Y\,(0) = p \tag{55}$$

If $x(t)$ is continuous then obviously $p = 0$ and derivative (54) also belongs to the hyperbolic algebra, otherwise the quantity p may serve for elimination of singularities as seen from equation (48).

As a simple application, consider the initial value problem

$$\begin{aligned} \dot{x} + \lambda x &= 2p\delta(t-a) = p\ddot{s} \\ x(0) &= 0 \end{aligned} \tag{56}$$

where λ and p are constant.

By considering functions $X\,(s)$ and $Y\,(s)$ in (52) as new unknowns, then substituting (52) through (54) in (56), and taking into account the linear independence of basis $\{1, \dot{s}\}$, gives

$$\begin{aligned} Y' + \lambda X &= 0 \\ X' + \lambda Y &= 0 \\ X(a) - Y(a) &= 0 \end{aligned} \tag{57}$$

under condition (55).

The boundary value problem (55) is free of δ-functions and admits an obvious solution , $X \equiv Y = p\exp(-\lambda s)$. Substituting these X- and Y-components in (52), gives solution of the initial value problem (56) in the form

$$x = p\exp(-\lambda s)(1 + \dot{s}) \tag{58}$$

The link established between nonsmooth temporal substitution (50) and the hyperbolic structure essentially facilitates analytical manipulations with differential equations. For example, instead of using the standard basis $\{1, \dot{s}\}$ it is

possible to introduce the so-called idempotent basis, associated with the two isotropic lines which separate the hyperbolic quadrants as follows

$$\begin{aligned} i_{\pm} &= \frac{1}{2}(1 \pm \dot{s}) \\ i_{\pm}^2 &= i_{\pm}, \quad i_{+}i_{-} = 0 \end{aligned} \tag{59}$$

Transition to the idempotent basis in (50) gives

$$t = (a+s)i_{+} + (a-s)i_{-} \tag{60}$$

Due to the properties of basis (59), substitution (60) possesses ‘functional linearity.’ In other words,

$$t^{\alpha} = (a+s)^{\alpha}i_{+} + (a-s)^{\alpha}i_{-} \tag{61}$$

for any real α, and generally,

$$\begin{aligned} x(t) &= x[(a+s)i_{+} + (a-s)i_{-}] \\ &= x(a+s)i_{+} + x(a-s)i_{-} \\ &\equiv X_{+}(s)i_{+} + X_{-}(s)i_{-} \end{aligned} \tag{62}$$

The advantage of the idempotent basis is that the differential equations of motion with respect to components X_{+} and X_{-} are decoupled. Instead the boundary conditions become coupled though. Different examples of solutions in the idempotent basis are given in recent publications [49] and [48].

3.2 Triangular sine-wave time substitution

Since any vibrating process is a sequence of U-turns then the corresponding nonsmooth time substitution can be combined of functions given by (43) with different signs and temporal shifts. In periodic case of the period $T = 4$, such combination is given by the sawtooth function (22), whose argument is replaced by time, $\tau = \tau(t)$. A mechanical model generating such time substitution by its free motion is shown in Fig. 12 (b) while the periodic version of identity (50) is

$$t = 1 + (\tau - 1)\,\dot{\tau} \qquad \text{if } -1 < t < 3 \tag{63}$$

where $\dot{\tau}^2 = 1$, and therefore (63) is a hyperbolic number with the basis $\{1, \dot{\tau}\}$.

In physical terms, it follows from (63) that any periodic process, whose period is normalized to $T = 4$, is uniquely expressed through the dynamic states of standard impact oscillator in the form [45]

$$x\,(t) = X\,(\tau) + Y\,(\tau)\,\dot{\tau} \tag{64}$$

where

$$\begin{aligned} X\,(\tau) &= \frac{1}{2}\left[x\,(\tau) + x\,(2-\tau)\right] \\ Y\,(\tau) &= \frac{1}{2}\left[x\,(\tau) - x\,(2-\tau)\right] \end{aligned} \tag{65}$$

Identity (64) means that the triangular sine and rectangular cosine waves capture temporal symmetries of periodic processes regardless specifics of individual vibrating systems.

Introducing a slow temporal scale in (64) extends the area of applications on modulated vibrating processes. In such cases, two variable expansions [27] can be used by considering the triangular sine time as a fast scale [48].

Different applications of nonsmooth argument substitutions with the related techniques to problems of theoretical and applied mechanics can be found in [47], [30], [32], [31], [16], [63], [29], [28], [55], [57], [53], [54], [52], [59], [37], [36], [60], [20]. The methodology was adapted also to the nonlinear normal mode analyses and included in monograph [64]. While the idea of NNMs is effective in case of weak or no energy exchange, the concept of the limiting phase trajectories [30] considers the opposite situation namely intense energy exchanges between weakly coupled oscillators or modes [32], [34], [33]. In this case, nonsmooth time substitutions are invoked by the temporal behavior of phase angle, which is responsible for energy distribution. This resembles the sawtooth wave as the energy swing reaches its asymptotic limit.

Very recently, a class of strongly nonlinear traveling waves and localized modes in one-dimensional homogeneous granular chains with no precompression were considered in [58]. In particular, the asymmetric version of identity (64) [42] was applied. As a result, the authors developed a systematic semi analytical approaches for computing different families of nonlinear traveling waves parametrized by spatial periodicity (wave number) and energy.

3.3 Quasi linear asymptotics for nonsmooth perturbations

There are many physical and mechanical models described by linear oscillators with small but nonsmooth perturbations. The related examples of mechanical oscillators were considered in reference [39]. Nonsmooth but still continuous characteristics of elastic forces often occur when modeling the dynamics of elastic structures with cracks [7], [6], [66]. More references and mathematical remarks on different cases of nonsmooth perturbations can be found in reference [5]. As a non-conservative case of nonsmooth perturbations, let us mention the following modification of Van der Pol's oscillator [26], [18]

$$\ddot{q} + \varepsilon(|q| - 1)\dot{q} + q = 0 \tag{66}$$

where ε is a small parameter.

Note that, using the nonsmooth term in (66), reduces the degree of nonlinearity as compared to the classical Van der Pol's model. A periodic limit cycle solution of equation (66) was obtained in [18] by taking into account the identity $|q| = \mathrm{sgn}(q)q$ in order to facilitate trigonometric expansions for the method of multiple scales. The following generalized model was considered in [5]

$$\ddot{q} + \varepsilon(|q| - 1)\dot{q} + (1 + \varepsilon\sigma)q = \varepsilon\lambda \sin t \tag{67}$$

where σ is a detuning parameter.

Recall that classical methods of asymptotic integration require perturbations to be as smooth as needed for deriving solutions of certain asymptotic order. In such cases, non-smooth argument substitutions may facilitate formulations for high-order asymptotic approximations. Moreover, firts-order asymptotic solution are obtained exactly in a closed form. Let us illustrate this remark on the one-degree-of-freedom oscillator

$$\ddot{q} + \omega^2 q = \varepsilon\omega^2\theta(q)q \tag{68}$$

where $\theta(q)$ is the Heaviside unit-step function.

The perturbation on the right-hand side of oscillator (68) is a continuous but non-smooth function of the coordinate q. Nevertheless, let us represent the first-order asymptotic solution in the form

$$\begin{aligned} q &= A\cos\varphi + \varepsilon q_1(\varphi) + O(\varepsilon^2) \\ \varphi &= \omega(1 + \varepsilon\gamma_1 + O(\varepsilon^2))t \end{aligned} \tag{69}$$

where $A = \mathit{const.} > 0$, and q_1 and γ_1 are yet unknown corrections to the generating solution obtained under the condition $\varepsilon = 0$.

Substituting (69) in (68) and matching first-order terms of ε on both sides of the equation, gives

$$\frac{d^2q_1}{d\varphi^2} + q_1 = A\cos\varphi[2\gamma_1 + \theta(\cos\varphi)] \tag{70}$$

where the amplitude A in the argument of unit-step function θ has been ignored as a positive factor of no influence on the output.

For further comparison reason, let us reproduce first solution of equation (70) in terms of trigonometric expansions. According to the idea of Poincare-Lindstedt method, the parameter γ_1 is determined by using Fourier series with respect to φ and eliminating the resonance term on the right-hand side of equation (70) that gives $\gamma_1 = -1/4$. The first-order approximation $q_1(\varphi)$ is obtained then in the form

$$\begin{aligned} q &= A\left[\cos\varphi + \frac{\varepsilon}{\pi}\left(1 - \frac{2}{9}\cos 2\varphi + \frac{2}{225}\cos 4\varphi + ...\right)\right] + O(\varepsilon^2) \\ \varphi &= \omega\left[1 - \frac{\varepsilon}{4} + O(\varepsilon^2)\right]t \end{aligned} \tag{71}$$

The error of solution (71) depends upon both the magnitude of ε and the number of terms retained in the Fourier series.

Now let us solve equation (70) by applying identity (64) to the right-hand side of equation (70) and its unknown 2π-periodic solution. In other words, let us represent solution in the form

$$\begin{aligned} q_1 &= X(\tau) + Y(\tau)e \\ \tau &= \tau(2\varphi/\pi) \\ e &= e(2\varphi/\pi) \equiv d\tau(2\varphi/\pi)/d(2\varphi/\pi) \end{aligned} \tag{72}$$

where X and Y are new unknown functions of the argument τ, and obviously $e^2 = 1$ for almost all φ.

Then, substituting (72) in (70) and taking into account the identities $\cos\varphi = \cos(\pi\tau/2)e$ and $\theta(\cos\varphi) = (1+e)/2$, gives

$$\left(\frac{2}{\pi}\right)^2 \frac{d^2X}{d\tau^2} + X = \frac{1}{2} A \cos\frac{\pi\tau}{2}, \quad \frac{dX}{d\tau}|_{\tau=\pm1} = 0 \tag{73}$$

$$\left(\frac{2}{\pi}\right)^2 \frac{d^2Y}{d\tau^2} + Y = \left(\frac{1}{2} + 2\gamma_1\right) A \cos\frac{\pi\tau}{2}, \quad Y|_{\tau=\pm1} = 0 \tag{74}$$

Recall that boundary conditions in (73)-(74) eliminate the singularities of differentiation caused by the formal presence of non-smooth functions in (72). It can be verified by inspection that problem (73) always admits a solution whereas problem (74) is solvable only under the condition $\gamma_1 = -1/4$. Note that this number is identical to that eliminates the resonance term on the right-hand side of equation (70). In the present procedure, however, the number $\gamma_1 = -1/4$ eliminates the 'imaginary' component from representation (72) due to the trivial solution of boundary value problem (74) whereas the 'real' component is easily determined from (73). As a result, first-order asymptotic solution (69) takes the closed form

$$\begin{aligned} q(t) &= A\left[\cos\varphi + \frac{\varepsilon}{8}\left(2\cos\frac{\pi\tau}{2} + \pi\tau\sin\frac{\pi\tau}{2}\right)\right] + O(\varepsilon^2) \\ \varphi &= \omega\left[1 - \frac{\varepsilon}{4} + O(\varepsilon^2)\right]t, \quad \tau = \tau\left(\frac{2\varphi}{\pi}\right) \end{aligned} \tag{75}$$

Note that solution (75) appears to have the so-called 'secular term' $\tau\sin(\pi\tau/2)$, which is bounded and periodic however with respect to the original temporal argument t.

In order to compare solutions (71) and (75), let us fix the amplitude parameter as $A = 1.0$ in (75) and then determine the corresponding amplitude parameter of solution (71) in order to achieve the same initial value $q(0)$. Then, selecting $\varepsilon = 0.25$ and keeping the three terms of Fourier expansion of order ε as shown in (71), gives a very good match of solutions (71) and (75) in terms of the coordinate q. This is due to quite a rapid convergence of the Fourier series in (71) as seen from its coefficients. However, since differentiation slows down the convergence then some mismatch in accelerations occurs between the two solutions as shown in Fig. 13. In the diagram, the dashed line represents numerical solution produced by the built-in Mathematica® solver.

3.4 Nonsmooth time decomposition

In this subsection, the original temporal argument t is replaced by a sequence of nonsmooth arguments $\{s_i\}$ $(i = 1, 2, ...)$ running within the same standard interval $0 \le s_i \le 1$. This brings advantage of using bounded time arguments and, as shown below, provides a convenient description of impulsively loaded

dynamical systems. As a mathematical basis, consider the ramp function,

$$s\left(t;d\right)=\frac{1}{2}\left(d+|t|-|t-d|\right) \tag{76}$$

and its first order generalized derivative, $\dot{s}\left(t;d\right)$, with respect to the temporal argument, t; see Figs.14 and 15, respectively.

Such kind of functions are quite common for signal analyses [25]. In our case, however, physical interpretation of these functions represented in Fig. 12 (c) are employed. Namely, the function $s\left(t,d\right)$ describes positions of a very small perfectly stiff bead located initially at the origin $x=0$ as shown by the dashed circle. The initial time instance $t=0$ associates with the event when this bead is struck on the left by the identical bead with the velocity $v=1$. Due to the linear momenta exchange, the reference bead starts moving by the law $x=x(t,d)$ until it hits the third bead located at $x=d=1$. Now, let us consider an infinite chain of perfectly stiff identical beads on a straight line at the points x_i $(i=0,1,...)$. As soon as no energy loss is assumed, any currently moving bead has the same velocity, $v=1$. As a result, the linear momentum is translated with the constant speed, whereas every bead moves only in between its two impact interactions with the neighbors. The motion of the ith bead is described by

$$s_i\left(t\right)=s\left(t-t_i,d_i\right)=\frac{1}{2}\left(d_i+|t-t_i|-|t-t_{i+1}|\right) \tag{77}$$

where t_i is the first interaction time of the ith bead, and $d_i=t_{i+1}-t_i$ is the time interval between its two consecutive interactions with its neighbors.

Due to the unit velocity, the variable s_i can play the role of 'local' time associated with the bead moving within the interval $x_i<x<x_{i+1}$ while the 'global' time t runs together with the linear momentum across the entire chain of beads. However, for any sequence of time instances, $\Lambda=\{t_0,t_1,...\}$, the global time, $t\in[t_0,\infty)$, can be expressed through the sequence of local times, $\{s_i\}$, in the form [44]

$$t=\sum_{i=0}^{\infty}\left(t_i+s_i\right)\dot{s}_i \tag{78}$$

where the basis $\{\dot{s}_i\}$ obeys the following table of products

$$\dot{s}_i\dot{s}_j=\dot{s}_i\delta_{ij} \tag{79}$$

As a result, the following 'functional linearity' property holds for quite a general process $x(t)$

$$x\left(t\right)=x\left(\sum_{i=0}^{\infty}\left(t_i+s_i\right)\dot{s}_i\right)=\sum_{i=0}^{\infty}x\left(t_i+s_i\right)\dot{s}_i \tag{80}$$

As mentioned at the beginning of this subsection, the area of applications of time substitution (78) includes impulsively loaded dynamical systems. In

particular, taking into account (80) and differentiation rules [44], eliminates the external impulses from dynamical system,

$$\begin{aligned} \dot{\mathbf{x}} &= \mathbf{f}(\mathbf{x}, t) + \sum_{i=0}^{\infty} \mathbf{p}_i \delta(t - t_i), \qquad \mathbf{x}(t) \in R^n \\ \mathbf{x} &\equiv 0, \qquad t < t_0 \end{aligned} \tag{81}$$

where $\mathbf{f}(\mathbf{x}, t)$ is regular vector-function and $\mathbf{p}_i$ are vectors characterizing magnitudes and directions of the impulses.

The new system is considered then in the local (bounded) time arguments $\{s_i\}$ by using general analytical tools such as Lie series expansions. Such approach was applied to the Duffing oscillator with no linear stiffness under sine modulated random impulses [44],

$$\ddot{x} + \zeta \dot{x} + x^3 = B \sin t \sum_{i=0}^{\infty} \delta(t - t_i) \tag{82}$$

where ζ is a constant linear damping coefficient, and B is the amplitude of modulation.

The distance between any two sequential impulse times is given by

$$d_i = t_{i+1} - t_i = \frac{\pi}{12}(1 + \beta \eta_i)$$

where η_i are random real numbers homogeneously distributed on the interval $[-1, 1]$, and β is a small positive number, $0 < \beta \ll 1$.

Introducing the state vector $\mathbf{x} = (x, \dot{x})^T \equiv (x_1, x_2)^T$, brings system (82) to the standard form (81), where

$$\mathbf{f}(\mathbf{x}) = \begin{pmatrix} x_2 \\ -\zeta x_2 - x_1^3 \end{pmatrix}, \quad \mathbf{p}_i = \begin{pmatrix} 0 \\ B \sin t_i \end{pmatrix}$$

Note that oscillator (82) is a modification of the well known oscillator, $\ddot{x} + \zeta \dot{x} + x^3 = B \sin t$, considered by Ueda [62] as a model of nonlinear inductor in electrical circuits. In particular, the result of work [62], as well as many further investigations of similar models, revealed the existence of stochastic attractors often illustrated by the Poincare diagrams. Similar diagrams obtained under irregular snapshots can be qualified as 'stroboscopic' diagrams. The results of the computer simulations [44] show that some irregularity of the pulse times can be used for the purposes of a more clear observation of the system orbits in the stroboscopic diagrams subjected to a chain of significant structural changes as the parameter B increases. When repeatedly executing the numerical code, under the same input conditions, such a small disorder in the input results some times in a less noisy and more organized stroboscopic diagrams. However, such phenomenon itself was found to be a random event whose 'appearance' depends on the level of pulse randomization as well as the number of iterations.

4 Concluding remarks

This work outlined very different ways to modeling dynamical systems with discontinuities by choosing proper spatial coordinates or temporal arguments within the class of nonsmooth functions. Note that nonsmooth transformation of state vector (38) can be viewed as a generalization of nonsmooth coordinate transformation (29). Whereas transformation (29) is conservative, transformation (38) possesses built in energy sinks pumping out some energy from the system whenever it crosses the image of the barrier in the unfolded space. In contrast to substitution (6), both substitutions (38) and (29) are essentially nonlinear and thus produce essentially nonlinear differential equations of motion even when out of constraints the equations of motion are linear. None of the above transformation affects the time variable. In contrast, the nonsmooth time substitutions described in Section 3 incorporate general temporal symmetries of dynamic processes. Although such symmetries develop most explicitly through natural motions of elementary impact models as shown in Fig. 12, the corresponding time substitutions impose no constrains on class of smoothness of those systems to which such substitutions are applied. One specific feature of the nonsmooth time substitutions is that they induce the hyperbolic structure of spatial coordinates. Further details on the related mathematical properties and physical interpretations are described in [48]. Finally note that it is possible to combine different transformations described in the present survey whenever technical reasons for such combinations are present; some examples can be found in [43] and [60].

References

[1] Split-complex number. *Wikipedia*.

[2] M. A. Aizerman and F. R. Gantmacher. On the stability of periodic motions. *Applied Mathematics and Mechanics (PMM)*, 22:781–788, 1958.

[3] K.V. Avramov. Application of nonsmooth transformations to analyze a vibroimpact duffing system. *International Applied Mechanics*, 44(10):1173–1179, 2008.

[4] V. I. Babitsky. *Theory of Vibroimpact Systems and Applications*. Springer-Verlag, Berlin, 1998.

[5] A. Buika, J. Llibre, and O. Makarenkov. Asymptotic stability of periodic solutions for nonsmooth differential equations with application to the nonsmooth van der pol oscillator. *arXiv*, 0709.4462v2, 2008.

[6] E. A. Butcher and R. Lu. Order reduction of structural dynamic systems with static piecewise linear nonlinearities. *Nonlinear Dynamics*, 49(3):375–399, 2007.

[7] S. Chen and S.W. Shaw. Normal modes for piecewise linear vibratory systems. *Nonlinear Dynamics*, 10:135–163, 1996.

[8] J. Cockle. A new imaginary in algebra. *London-Edinburgh-Dublin Philosophical Magazine*, ((3) 33:345-9), 1848.

[9] M. F. Dimentberg. *Statistical Dynamics of Nonlinear and Time-Varying Systems*. John Wiley & Sons, New York, 1988.

[10] M. F. Dimentberg and D. V. Iourtchenko. Stochastic and/or chaotic response of a vibration system to imperfectly periodic sinusoidal excitation. *International Journal of Bifurcation and Chaos*, 15(6):2057–2061, 2005.

[11] M.F. Dimentberg, O. Gaidai, and A. Naess. Random vibrations with strongly inelastic impacts: Response pdf by the path integration method. *International Journal of Non-Linear Mechanics*, 44(7):791 – 796, 2009.

[12] M.F. Dimentberg and A.I. Menyailov. *Statistical Dynamics of Nonlinear and Time-Varying Systems*. Research Studies Press, Taunton UK, 1988.

[13] A. Fidlin. *Nonlinear Oscillations in Mechanical Engineering*. Springer, Berlin Heidelberg, 2005.

[14] A. F. Filippov. *Differential equations with discontinuous righthand sides*. Kluwer Academic Publishers Group, Dordrecht, 1988. Translated from the Russian.

[15] S. Fucik and A. Kufner. *Nonlinear differential equations*. Elsevier, Amsterdam, Oxford, New York, 1980. Studies in Applied Mechanics 2, Elsevier Scientific Publishing Company.

[16] O. Gendelman, L. I. Manevitch, A. F. Vakakis, and R. M'Closkey. Energy pumping in nonlinear mechanical oscillators. I. Dynamics of the underlying Hamiltonian systems. *Trans. ASME J. Appl. Mech.*, 68(1):34–41, 2001.

[17] S. Haller and G. Hormann. Comparison of some solution concepts for linear first-order hyperbolic differential equations with non-smooth coefficients. *Publications De Linstitut Mathematique, Nouvelle serie*, 84(98):123–157, 2008.

[18] S. J. Hogan. Relaxation oscillations in a system with a piecewise smooth drag coefficient. *Journal Sound Vibration*, 263(2):467 – 471, 2003.

[19] J. Hucks. Hyperbolic complex structures in physics. *Journal of Mathematical Physics*, 34:5986, 1993.

[20] R.A. Ibrahim. *Vibro-Impact Dynamics: Modeling, Mapping and Applications, LNACM 43.* Springer-Verlag, Berlin, Heidelberg, 2009.

[21] A. P. Ivanov. Analytical methods in the theory of vibro-impact systems. *J. Appl. Maths. Mechs.*, 57(2):221–236, 1993.

[22] A. P. Ivanov. Bifurcations in impact systems. *Chaos, Solitons and Fractals*, 7(10):1615–1634, 1996.

[23] A. P. Ivanov. *Dynamics of Systems with Mechanical Collisions.* International Program of Education, Moscow, 1997. in Russian.

[24] A.P. Ivanov. Impact oscillations: linear theory of stability and bifurcations. *Journal of Sound and Vibration*, 178(3):361–378, 1994.

[25] L.B. Jackson. *Signals, Systems, and Transforms.* Addison-Wesley Publishing Company, New York, 1991.

[26] D.W. Jordan and P. Smith. *Nonlinear Ordinary Differential Equations. An Introduction to Dynamical Systems, 3rd Edition.* Oxford University Press, Oxford, 1999.

[27] J. Kevorkian and J. D. Cole. *Multiple scale and singular perturbation methods.* Springer-Verlag, New York, 1996.

[28] Y. S. Lee, F. Nucera, A. F. Vakakis, D.M. McFarland, and L. A. Bergman. Periodic orbits, damped transitions and targeted energy transfers in oscillators with vibro-impact attachments. *Physica D*, 238(18):1868 – 1896, 2009.

[29] Y.S. Lee, G. Kerschen, A.F. Vakakis, P. Panagopoulos, L. Bergman, and D.M. McFarland. Complicated dynamics of a linear oscillator with a light, essentially nonlinear attachment. *Physica D*, 204:41–69, 2005.

[30] L.I. Manevich. New approach to beating phenomenon in coupled nonlinear oscillatory chains. *Archive of Applied Mechanics*, 77:301–312, 2007.

[31] L. I. Manevitch and O.V. Gendelman. Oscillatory models of vibro-impact type for essentially non-linear systems. *Proceedings of the Institution of Mechanical Engineers, Part C: Journal of Mechanical Engineering Science (DOI: 10.1243/09544062JMES1057)*, 222(10):2007–2043, 2008.

[32] L. I. Manevitch and A.I. Musienko. Limiting phase trajectory and beating phenomena in systems of coupled nonlinear oscillators. *2nd International Conference on Nonlinear Normal Modes and Localization in Vibrating Systems, Samos, Greece, June 19-23*, pages 25–26, 2006.

[33] L.I. Manevitch, A.S. Kovaleva, and D.S. Shepelev. Non-smooth approximations of the limiting phase trajectories for the duffing oscillator near 1:1 resonance. *Physica D: Nonlinear Phenomena*, 240(1):1 – 12, 2011.

[34] L.I. Manevitch and V.V. Smirnov. Resonant energy exchange in nonlinear oscillatory chains and limiting phase trajectories: from small to large systems. *arXiv*, 0903.5455v1, 2009.

[35] V. P. Maslov and G. A. Omel′janov. Asymptotic soliton-like solutions of equations with small dispersion. *Uspekhi Mat. Nauk*, 36(3):63–126, 1981.

[36] Yu. V. Mikhlin and S. N. Reshetnikova. Dynamical interaction of an elastic system and a vibro-impact absorber. *Mathematical Problems in Engineering*, 2006(Article ID 37980):15 pages, 2006.

[37] Yu. V. Mikhlin and A. M. Volok. Solitary transversal waves and vibro-impact motions in infinite chains and rods. *International Journal of Solids and Structures*, 37:3403–3420, 2000.

[38] N. Sri Namachchivaya and Jun H. Park. Stochastic dynamics of impact oscillators. *Journal of Applied Mechanics*, 72(6):862–870, 2005.

[39] A. H. Nayfeh and D. T. Mook. *Nonlinear oscillations.* Wiley-Interscience, New York, 1979.

[40] V. N. Pilipchuk. The calculation of strongly nonlinear systems close to vibroimpact systems. *Journal of Applied Mathematics and Mechanics*, 49(5):572–578, 1985.

[41] V. N. Pilipchuk. Transformation of the vibratory-systems by means of a pair of nonsmooth periodic-functions. *Dopovidi Akademii Nauk Ukrainskoi RSR. Seriya A - Fiziko-Matematichni Ta Technichni Nauki (in Ukrainian)*, 4:36–38, 1988.

[42] V. N. Pilipchuk. Application of special nonsmooth temporal transformations to linear and nonlinear systems under discontinuous and impulsive excitation. *Nonlinear Dynam.*, 18(3):203–234, 1999.

[43] V. N. Pilipchuk. Non-smooth spatio-temporal transformation for impulsively forced oscillators with rigid barriers. *J. Sound Vibration*, 237(5):915–919, 2000.

[44] V. N. Pilipchuk. Non-smooth time decomposition for nonlinear models driven by random pulses. *Chaos Solitons Fractals*, 14(1):129–143, 2002.

[45] V. N. Pilipchuk. Temporal transformations and visualization diagrams for nonsmooth periodic motions. *International Journal of Bifurcation and Chaos*, 15(6):1879–1899, 2005.

[46] V. N. Pilipchuk and R. A. Ibrahim. Dynamics of a two-pendulum model with impact interaction and an elastic support. *Nonlinear Dynamics*, 21(3):221–247, 2000.

[47] V. N. Pilipchuk and G.A. Starushenko. A version of non-smooth transformations for one-dimensional elastic systems with a periodic structure. *Journal of applied mathematics and mechanics (PMM)*, 61(2):265–274, 1997.

[48] Valery N. Pilipchuk. *Nonlinear Dynamics: Between Linear and Impact Limits (Lecture Notes in Applied and Computational Mechanics)*. Springer, 2010.

[49] V.N. Pilipchuk. Closed form periodic solutions for piecewise-linear vibrating systems. *Nonlinear Dynamics*, http://dx.doi.org/10.1007/s11071-009-9469-0, 2009.

[50] R. D. Richtmyer. *Principles of Advanced Mathematical Physics*. Springer, Berlin, 1985.

[51] Haiwu Rong, Wei Wang, Xiangdongand Xu, and Tong Fang. Subharmonic response of a single-degree-of-freedom nonlinear vibroimpact system to a randomly disordered periodic excitation. *Journal of Sound and Vibration*, 327(1-2):173 – 182, 2009.

[52] G. Salenger, A. F. Vakakis, Oleg Gendelman, Leonid Manevitch, and Igor Andrianov. Transitions from strongly to weakly nonlinear motions of damped nonlinear oscillators. *Nonlinear Dynam.*, 20(2):99–114, 1999.

[53] G. D. Salenger and A. F. Vakakis. Discreteness effects in the forced dynamics of a string on a periodic array of non-linear supports. *International Journal of Non-Linear Mechanics*, 33(4):659–673, 1998.

[54] G. D. Salenger and A. F. Vakakis. Localized and periodic waves with discreteness effects. *Mech. Res. Comm.*, 25(1):97–104, 1998.

[55] G. Sheng, R. Dukkipati, and J. Pang. Nonlinear dynamics of sub-10 nm flying height air bearing slider in modern hard disk recording system. *Mechanism and Machine Theory*, 41:1230–1242, 2006.

[56] G. Sobczyk. The hyperbolic number plane. *The College Mathematics Journal*, 26(4):268–280, 1995.

[57] D. S. Sophianopoulos, A. N. Kounadis, and A. F. Vakakis. Complex dynamics of perfect discrete systems under partial follower forces. *Internat. J. Non-Linear Mech.*, 37(6):1121–1138, 2002.

[58] Yu. Starosvetsky and A. F. Vakakis. Traveling waves and localized modes in one-dimensional homogeneous granular chains with no precompression. *Phys. Rev. E*, 82(2, Part 2):026603, AUG 20 2010.

[59] G. Starushenko, N. Krulik, and S. Tokarzewski. Employment of non-symmetrical saw-tooth argument transformation method in the elasticity theory for layered composites. *International Journal of Heat and Mass Transfer*, 45:3055–3060, 2002.

[60] J. J. Thomsen and A. Fidlin. Near-elastic vibro-impact analysis by discontinuous transformations and averaging. *Journal of Sound and Vibration*, 311:386–407, 2008.

[61] R. Tucker. *Mathematical Papers by William Kingdon Clifford.* AMS Chelsea Publishing, Providence, Rhode Island, 2007.

[62] Y. Ueda. Randomly transitional phenomena in the system governed by Duffing's equation. *J. Statist. Phys.*, 20(2):181–196, 1979.

[63] A. F. Vakakis and T. M. Atanackovic. Buckling of an elastic ring forced by a periodic attay of compressive loads. *ASME Journal of Applied Mechanics*, 66(June):361–367, 1999.

[64] A. F. Vakakis, L. I. Manevitch, Yu. V. Mikhlin, V. N. Pilipchuk, and A. A. Zevin. *Normal modes and localization in nonlinear systems.* John Wiley & Sons Inc., New York, 1996. A Wiley-Interscience Publication.

[65] E. G. Vedenova, L. I. Manevich, and V. N. Pilipchuk. Normal oscillations of a string with concentrated masses on nonlinearly elastic supports. *Prikl. Mat. Mekh.*, 49(2):203–211, 1985.

[66] F. Vestroni, A. Luongo, and A. Paolone. A perturbation method for evaluating nonlinear normal modes of a piecewise linear two-degrees-of-freedom system. *Nonlinear Dynamics*, 54(4):379–393, 2008.

[67] V. S. Vladimirov. *Equations of mathematical physics (Monographs and textbooks in pure and applied mathematics, Vol.3).* M. Dekker, 1971.

[68] G. B. Whitham. *Linear and nonlinear waves.* John Wiley & Sons Inc., New York, 1999. Reprint of the 1974 original, A Wiley-Interscience Publication.

[69] V. F. Zhuravlev. A method for analyzing vibration-impact systems by means of special functions. *Izvestiya AN SSSR Mekhanika Tverdogo Tela (Mechanics of Solids)*, 11(2):30–34, 1976.

[70] V. F. Zhuravlev. Equations of motion of mechanical systems with ideal one-sided links. *Prikl. Mat. Mekh.*, 42(5):781–788, 1978.

[71] V. F. Zhuravlev and D. M. Klimov. *Prikladnye metody v teorii kolebanii*. "Nauka", Moscow, 1988. Edited and with a foreword by A. Yu. Ishlinskiĭ.

FIGURE CAPTIONS

Fig. 1: Temporal shapes of the force applied to the unit mass δ_ε and the corresponding velocity θ_ε for $\varepsilon = 0.5$.

Fig. 2: Impulse produced by the 'product' of unit-step and Dirac delta functions versus the model parameter.

Fig.3: Equipotential energy levels in the unfolded configuration plane and a sample dynamic trajectory obtained under the initial conditions at $t = 0$: $x_1 = 0.5$, $x_2 = 0.0$, $\dot{x}_1 = 1.0$, and $\dot{x}_2 = 0.0$.

Fig. 4: The beat-wise impact dynamics of the first mass in its original coordinate.

Fig. 5: The beat-wise impact dynamics of the second mass in its original coordinate; the energy exchange between the two masses is seen from the phase shift in their time histories.

Fig. 6: The impact mode trajectories in the unfolded configuration plane: in-phase and out-of-phase modes (the diagonal lines), and local modes (the horizontal and vertical lines.)

Fig. 7: A family of phase trajectories of the oscillator with one-sided barrier at different energy levels for the case $P(q) = q^2/2$.

Fig. 8: The phase trajectory of inelastic impact oscillator in the auxiliary coordinates.

Fig. 9: The original phase plane of the harmonic oscillator with a perfectly stiff but inelastic one-sided barrier.

Fig. 10: A classic particle reflected by smooth potential barrier.

Fig. 11: The nonsmooth temporal argument s and the particle' motion, $x(t)$.

Fig. 12: Three basic impact models generating nonsmooth time substitutions: (a) positive time, (b) triangular sine-wave time, and (c) nonsmooth time decomposition.

Fig. 13: Acceleration curves: Poincare-Lindstedt method (thin line), nonsmooth time substitution (thick line), and numerical (dashed line); $\omega = 1.0$, and $\varepsilon = 0.25$.

Fig. 14: The unit slope ramp function at $d = 1.0$.

Fig. 15: First derivative of the ramp function

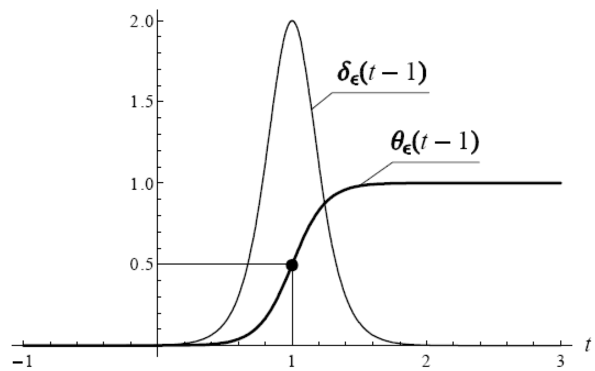

Figure 1: Temporal shapes of the force applied to the unit mass δ_ε and the corresponding velocity θ_ε for $\varepsilon = 0.5$.

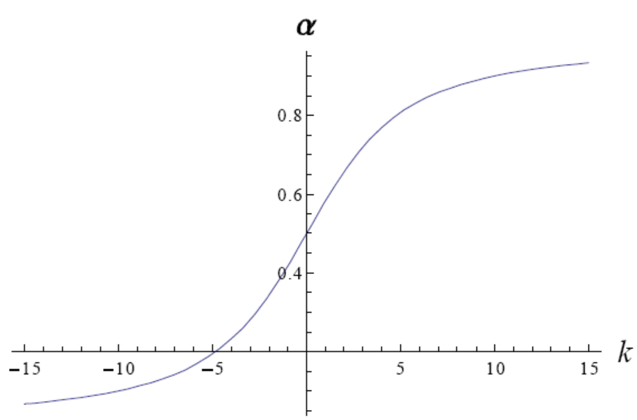

Figure 2: Impulse produced by the 'product' of unit-step and Dirac delta functions versus the model parameter.

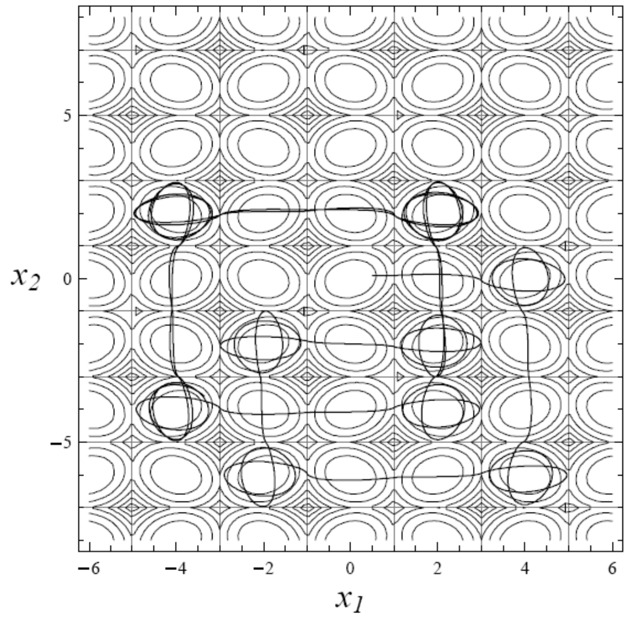

Figure 3: Equipotential energy levels in the unfolded configuration plane and a sample dynamic trajectory obtained under the initial conditions at $t = 0$: $x_1 = 0.5$, $x_2 = 0.0$, $\dot{x}_1 = 1.0$, and $\dot{x}_2 = 0.0$.

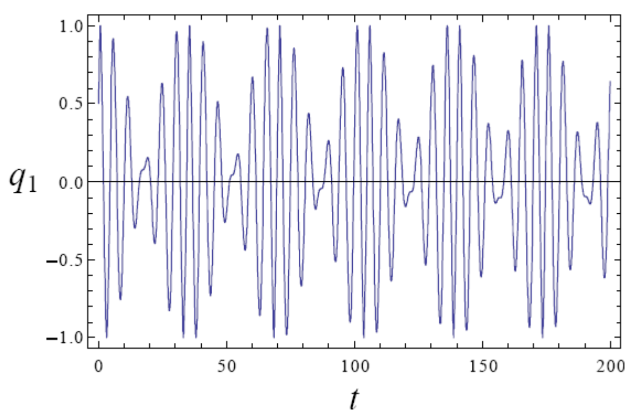

Figure 4: The beat-wise impact dynamics of the first mass in its original coordinate.

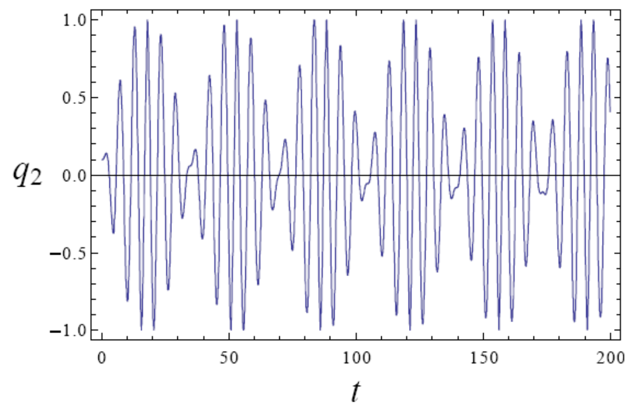

Figure 5: The beat-wise impact dynamics of the second mass in its original coordinate; the energy exchange between the two masses is seen from the phase shift in their time histories.

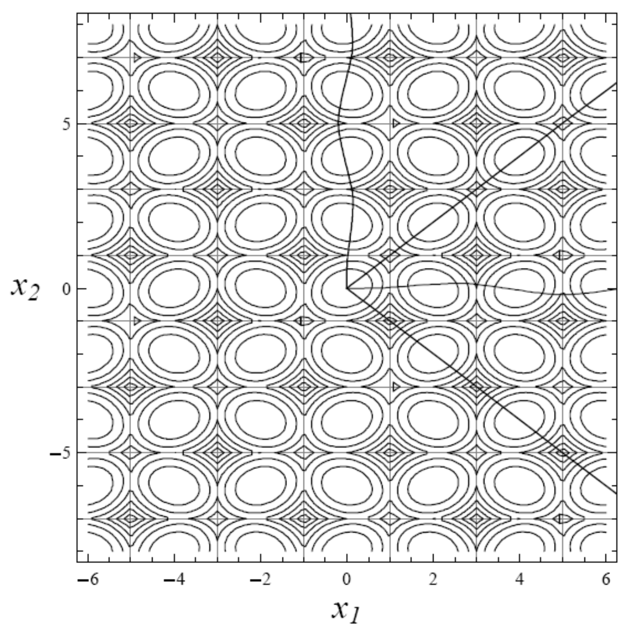

Figure 6: The impact mode trajectories in the unfolded configuration plane: in-phase and out-of-phase modes (the diagonal lines), and local modes (the horizontal and vertical lines.)

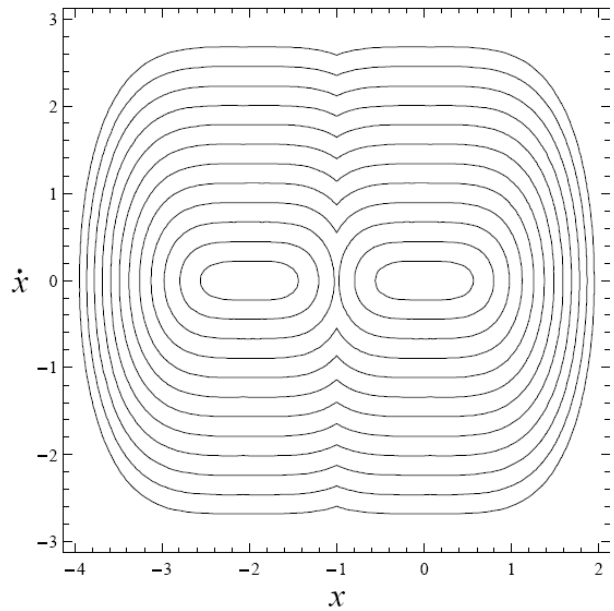

Figure 7: A family of phase trajectories of the oscillator with one-sided barrier at different energy levels for the case $P(q) = q^2/2$.

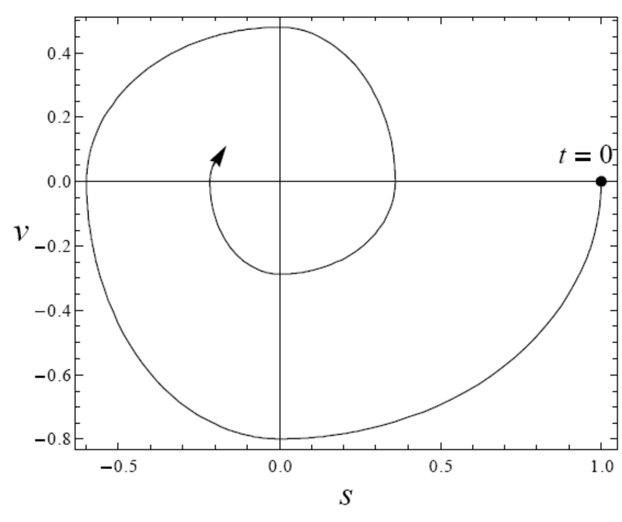

Figure 8: The phase trajectory of inelastic impact oscillator in the auxiliary coordinates.

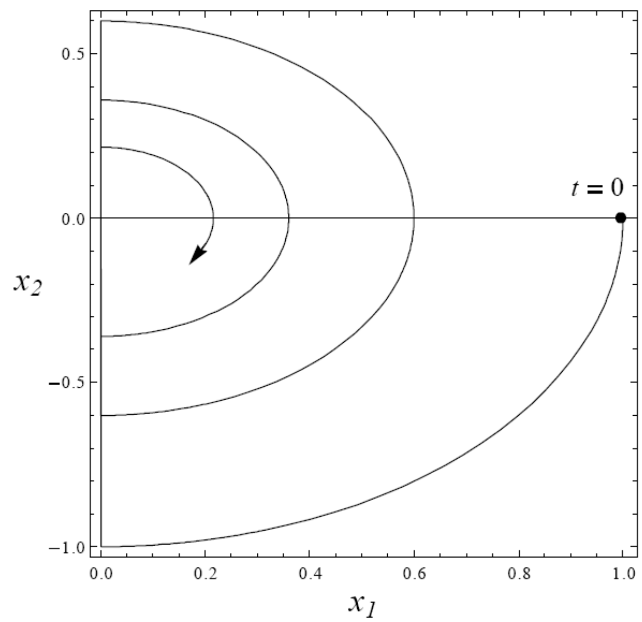

Figure 9: The original phase plane of the harmonic oscillator with a perfectly stiff but inelastic one-sided barrier.

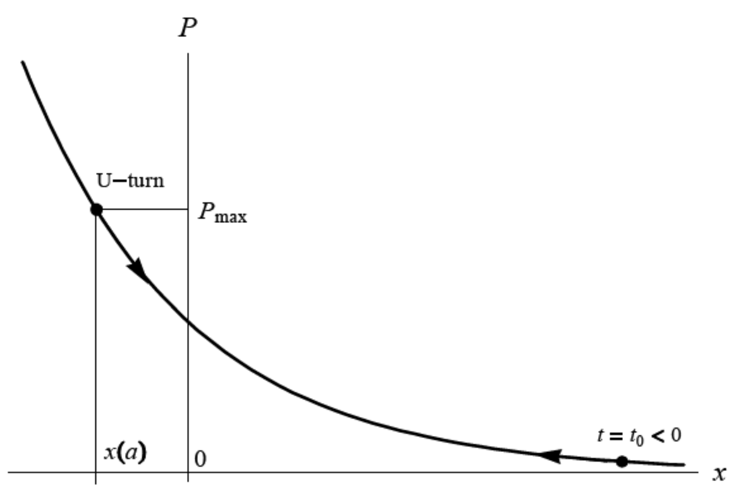

Figure 10: A classic particle reflected by smooth potential barrier.

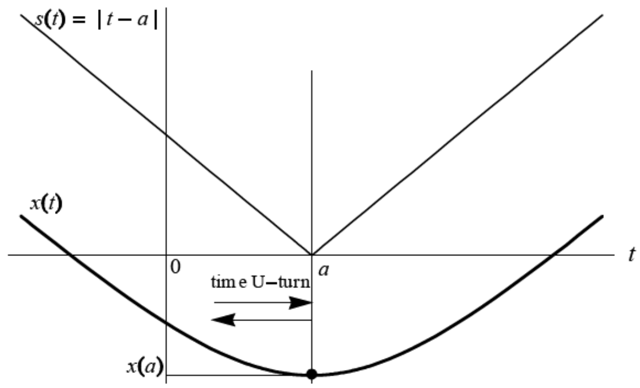

Figure 11: The nonsmooth temporal argument s and the particle' motion, $x(t)$.

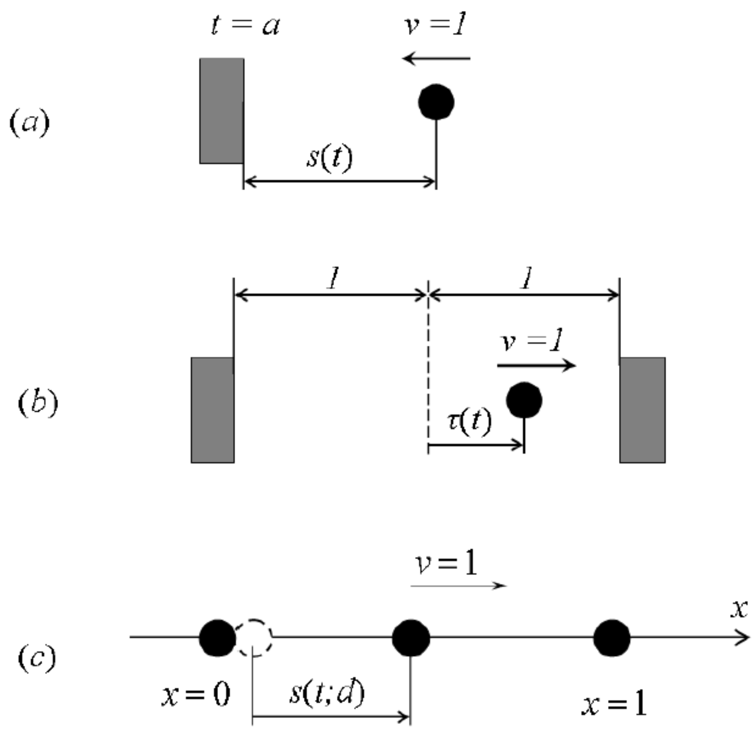

Figure 12: Three basic impact models generating nonsmooth time substitutions: (a) positive time, (b) triangular sine-wave time, and (c) nonsmooth time decomposition.

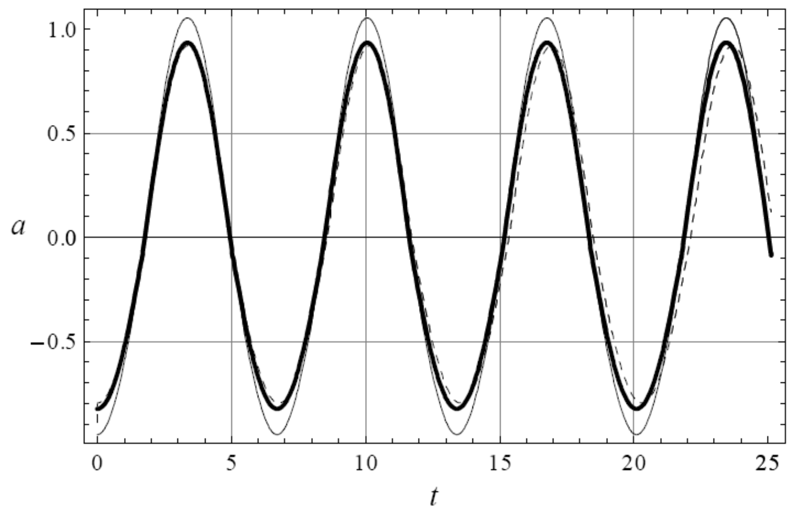

Figure 13: Acceleration curves: Poincare-Lindstedt method (thin line), non-smooth time substitution (thick line), and numerical (dashed line); $\omega = 1.0$, and $\varepsilon = 0.25$.

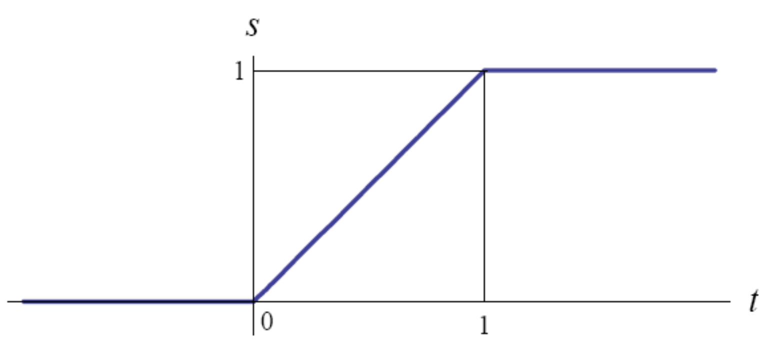

Figure 14: The unit slope ramp function at $d = 1.0$

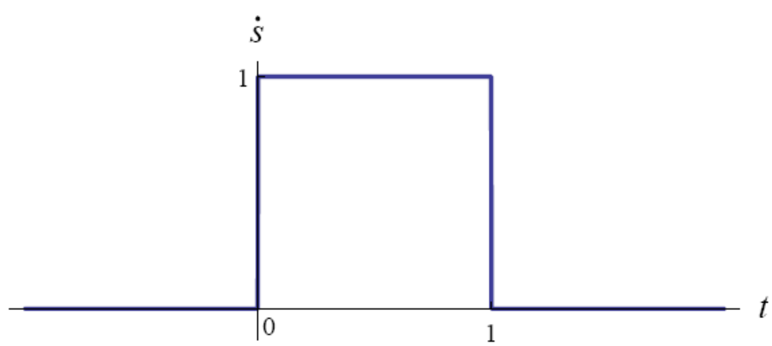

Figure 15: First derivative of the ramp function